Geometric Links Among Classical Controls Tools

T. R. Kurfess and M. L. Nagurka

Abstract— **This paper develops a geometric perspective that ties together a number of graphically based techniques from classical control theory. In particular, in the frequency domain, a connection between the Nyquist diagram and the Bode plots is unfolded via a sequence of three-dimensional representations. A parallel development in the "gain-domain" begins with the Evans root locus plot and leads to a set of gain plots that portray eigenvalue behavior as an explicit function of forward gain. The gain plots extend the standard root locus plot by depicting explicitly the influence of gain (or any system parameter) on the closed-loop system eigenvalues. This is similar to the way the Bode plots embellish the information of the Nyquist diagram by exposing frequency explicitly. The gain plots enable direct determination of gain values for which the closed-loop system is stable or unstable. By exposing the correspondence of gain values to specific eigenvalues, the plots serve as a pole-placement tool for identifying closed-loop designs meeting performance specifications. Furthermore, the gain plots reveal by inspection information about the closed-loop root sensitivity. We have found the gain plots as well as the underlying geometric development in both the frequency and gain domains invaluable in undergraduate and graduate controls education.**

I. Introduction

IN A SEQUENCE of landmark papers, W. R. Evans [1], [2] presented a technique for analyzing and graphically portraying the loci of closed-loop system poles. Since the publication of these papers, the Evans root locus technique has become a standard and commonly employed tool of the control engineer. The root locus plot has several qualities that make it a valuable classical controls tool, including the ease with which it may be implemented and the tremendous amount of information and insight that it provides.

For most single-input, single-output (SISO) linear time-invariant systems, sketching the root locus as a function of gain is a simple and well-documented task. Most undergraduate controls textbooks [3]–[6] present the sketching rules for constructing the root locus plot. By following these rules, the loci of roots or system eigenvalues may be graphed in the complex plane as a parameter is varied. Although the rules are applicable to any real valued parameters, the most common parameter investigated is the proportional control gain. This paper promotes an alternate graphic representation of the root locus plot that exposes the explicit relationship between the pole locations and the gain (without sacrificing any of the information presented in the standard root locus.)

Manuscript received December 1991.This work was supported in part by the National Science Foundation grant no. DUE9255567.

T. R. Kurfess is with the departments of Mechanical Engineering and Engineering and Public Policy, Carnegie Mellon University, Pittsburgh, PA 15213.

M. L. Nagurka is with the Department of Mechanical Engineering, Carnegie Mellon University, Pittsburgh, PA 15213.

IEEE Log Number 9214224.

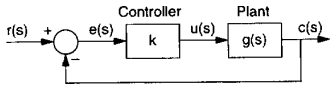

Fig. 1. Closed-loop SISO negative feedback configuration.

The representation, based on the same variable gain analysis employed by Evans, is summarized in a pair of gain plots that casts the magnitude and angle of the system eigenvalues in the complex plane as a function of gain. By utilizing an eigenvalue polar representation, the gain plots present system performance-related information, such as damping ratio and natural frequency, and, as such, serve as a graphic pole-placement tool. Additionally, sensitivity of the closed-loop eigenvalues with respect to gain can be obtained by examining the slopes of the gain plots.

Although gain plots are applicable to multivariable systems [7], [8], this paper specifically addresses SISO systems as covered in "classical controls." For purposes of illustration, the system represented by the open-loop transfer function, g(s),

$$g(s) = \frac{(s+3)}{(s+1)(s+2)} \tag{1}$$

is used as a theme example problem in the following two sections. This transfer function is embedded in a standard closed-loop negative feedback system shown in Fig. 1.

The paper is organized as follows. A conceptual framework that motivates the development of the gain plots is presented in the next two sections. First, the development of classical *frequency-domain* techniques is unfolded via a sequence of three-dimensional representations; then, in parallel fashion, a progression of *gain-domain* methods is identified. A subsequent section describes properties and advantages of gain plots that make them a rich design tool. A nontrivial SISO example, demonstrating the utility of the gain plots for stability, performance, and root sensitivity analyses, is then solved. Finally, a high-level perspective that integrates the gain plots with three key classical control tools is suggested.

II. Frequency-Domain Conceptualization

This section promotes a unifying framework for viewing classical control frequency-domain tools, such as the Nyquist diagram and Bode plots. The premise is that the Bode plots present the information of the Nyquist diagram in an enhanced perspective by exposing frequency explicitly. Furthermore, the Bode plots are the result of a natural progression of perspectives of the classical Nyquist diagram. Although this progression does not necessarily reflect the chronological unfolding of events, it serves as a useful paradigm that

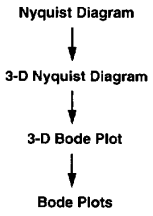

Fig. 2. Progression of frequency-domain tools.

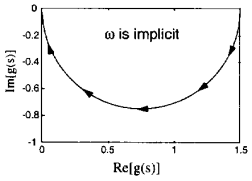

Fig. 3. The Nyquist diagram of (1).

logically bridges the fundamental frequency-domain tools of classical controls. This transition from the Nyquist diagram to two different three-dimensional representations, including one that reveals the classical Bode plots via orthogonal views, is summarized in Fig. 2.

Later in this paper, it is shown that this development of the Bode plots from the Nyquist diagram is paralleled by the development of the gain plots from the Evans root locus plot. As such, fundamental geometric relationships appear to exist among the Nyquist diagram, the Bode plots, the Evans root locus, and the gain plots.

2.1 The Nyquist Diagram

The Nyquist diagram [9] is a polar plot of a sinusoidal transfer function, $g(j\omega)$, graphed over the range $0 \leq \omega \leq \infty$. (The lower limit of the range can alternatively be chosen as $-\infty$, with the resulting curve being symmetric about the real axis.) Although the Nyquist diagram is a polar representation, it is graphed in a complex Cartesian plane where the implicit variable is ω. Fig. 3 is the Nyquist diagram of (1). The Nyquist curve starts at $\omega = 0$ corresponding to a dc gain of 1.5 and phase angle of 0°, and asymptotically approaches the origin (zero magnitude) from $-90°$.

It is possible to show the frequency graduation on the locus (with tick marks denoting equal values of ω) or to present superimposed constant frequency contours [5]. However, even if these are added, it is not convenient to identify the frequency associated with a given point on the Nyquist diagram.

2.2 Three-Dimensional Nyquist Diagram

The Nyquist diagram can be conceptualized as a two-dimensional "collapsed" perspective of a three-dimensional curve, as shown in Fig. 4 for the transfer function of (1). In this representation, two of the axes remain the same as in the Nyquist diagram, i.e., real and imaginary components, and a third axis is added to denote the frequency, ω. Note that as $\omega \rightarrow \infty$, the curve approaches the origin of the complex plane. Although the three-dimensional curve is one means to incorporate frequency information into the Nyquist diagram, it

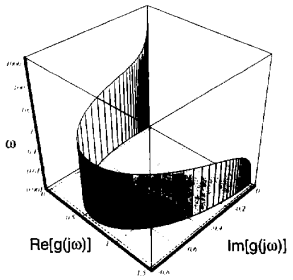

Fig. 4. Three-dimensional Nyquist diagram of (1).

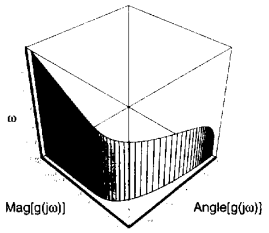

Fig. 5. Three-dimensional Bode plot of (1).

does not present the controls engineer with an intuitive feel for system behavior, partly because of the difficulty in following the contour and in extracting coordinate information.

2.3 Three-Dimensional Bode Plot

An alternative three-dimensional representation can be conceptualized that maps the real and complex components of $g(s)$ to magnitude and angle components. Here, the complex transfer function, $g(s)$, is written as

$$g(s) = Re[g(s)] + jIm[g(s)] = |g(s)|e^{j\angle g(s)} \tag{2}$$

where the transfer function angle and magnitude are given, respectively, as

$$\angle g(s) = \tan^{-1}(Im[g(s)], Re[g(s)]) \tag{3}$$

$$|g(s)| = \sqrt{\{Re[g(s)]\}^2 + \{Im[g(s)]\}^2} \tag{4}$$

where $\angle g(s)$ in (3) is given by the two argument inverse tangent function.

Equations (3) and (4) can be used to transform Fig. 4 into Fig. 5, showing the effect of frequency on the magnitude and angle of the open-loop system given by (1). Fig. 5 is a three-dimensional extension of well-known frequency plots, the Bode plots.

2.4 The Bode Plots

The Bode plots [10] consist of two planar plots, one being the Bode magnitude plot showing magnitude *vs.* frequency, and the second being the Bode angle (or phase) plot reporting angle versus frequency. Fig. 6 shows the Bode magnitude and angle plots for the open-loop system given by (1).

The Bode plots represent two orthogonal views of the three-dimensional Bode plot of Fig. 5, i.e., the Bode magnitude plot is seen by observing Fig. 5 from a direction orthogonal to the ω-magnitude plane and the Bode angle plot is seen

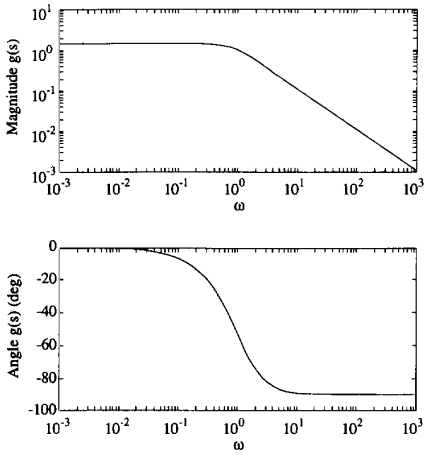

Fig. 6. Magnitude and angle Bode plots of (1).

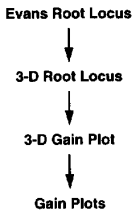

Fig. 7. Progression of gain-domain tools.

by viewing Fig. 5 from a direction orthogonal to the ω-angle plane. (In fact, Figs. 5 and 6 were generated using the identical data set.) Although the same information is presented in Figs. 5 and 6, the traditional Bode plots are significantly simpler to understand. Also, by viewing Fig. 5 from a direction orthogonal to the magnitude-angle plane the Nichols plot may be seen. Additional insightful geometric perspectives, such as those offered by generalized Bode diagrams, have been proposed in the literature [11], [12].

III. Gain-Domain Conceptualization

In an analogous fashion to the frequency-domain progression, the development of the gain plots follows a gain-domain evolution beginning with the Evans root locus plot. The traditional two-dimensional root locus plot is then complemented by a third axis representing gain. The resulting three-dimensional plot is conformally mapped into a new space, from which the gain plots can be viewed via two orthogonal perspectives. A summary of this development is traced in Fig. 7.

3.1 The Evans Root Locus

The root locus plot [1], [2] drawn in the complex plane shows the location of the characteristic roots, i.e. the eigenvalues, in terms of some (real valued) system parameter, such as the proportional gain. It is based on the closed-loop transfer function of Fig. 1 given by

$$g_{CL}(s) = \frac{k\,g(s)}{1 + k\,g(s)} \tag{5}$$

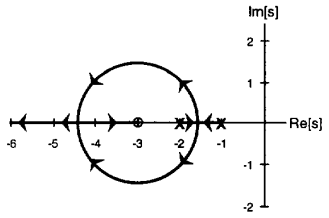

Fig. 8. Evans root locus plot of (1).

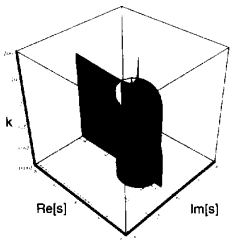

Fig. 9. Three-dimensional root locus plot of (1).

where k is a proportional gain. The stability of the closed-loop system is determined by the eigenvalues, i.e., the denominator roots of (5). The root locus is the solution set of

$$k\,g(s) = -1 \tag{6}$$

as the gain k varies in the range $0 \leq k < \infty$. Equation (6) is equivalent to two conditions: the angle criterion

$$\angle kg(s) = \pm 180°(2m+1), \quad m = 0, 1, 2, \ldots \tag{7}$$

and the magnitude criterion

$$|kg(s)| = 1 \tag{8}$$

The shape of the root locus plot is determined entirely by the angle criterion. Then, for any eigenvalue s on the root locus, the magnitude criterion is invoked to solve for the corresponding value of k. (This process is referred to as scaling the locus.) Fig. 8 is the root locus plot of (1) for the given range of k. Each branch of the root locus starts at $k = 0$ corresponding to a system open-loop pole, and asymptotically approaches either a finite or infinite transmission zero. It is possible to show the gain graduation on the locus (with tick marks denoting equal values of k) or to present superimposed constant gain contours.

3.2 Three-Dimensional Root Locus

In similar fashion to the way the Nyquist diagram was extended by adding a third frequency axis, the Evans root locus plot can be presented in three-dimensional space with the real and imaginary s-plane axes and a third gain axis. Fig. 9 presents such a three-dimensional root locus for the closed-loop system of Fig. 1 with open-loop transfer function of (1). The Evans root locus is the projection of this three-dimensional locus onto the real-imaginary plane.

The idea of adding a third dimension for gain is suggested in the literature [11]–[13]. It is useful for depicting a break-point as a saddle point. For example, two saddle points may be seen in Fig. 9. However, as before, the portrayal of three-dimensional information does not provide the controls engineer with an intuitive feel for system behavior.

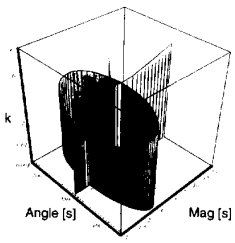

Fig. 10. Three-dimensional gain plot of (1).

3.3 Three-Dimensional Gain Plots

The three-dimensional representation described above can be viewed alternatively by mapping the real and complex components to magnitude and angle components. Here, the complex value, s, is expressed as

$$s = \sigma + j\omega = Re^{j\theta} \tag{9}$$

where the angle, θ, and magnitude, R, are

$$\theta = \tan^{-1}(\omega, \sigma) \tag{10}$$

$$R = \sqrt{\sigma^2 + \omega^2} \tag{11}$$

In (10) θ is given by the two argument inverse tangent function.

Equations (10) and (11) can be used to transform Fig. 9 into Fig. 10 showing the effect of gain on the magnitude and angle of the closed-loop system. Although difficult to visualize, this three-dimensional curve is related to the root-locus diagram.

3.4 The Gain Plots

Just as two-dimensional Bode plots simplify the three-dimensional Bode plot, two-dimensional gain plots may be employed to simplify the three-dimensional gain plot. Fig. 11 is such a representation, showing the magnitude and angle gain plots for the closed-loop system. The magnitude gain plot is seen by viewing Fig. 10 from a direction orthogonal to the k-magnitude plane and the angle gain plot is seen by observing Fig. 10 from a direction orthogonal to the k-angle plane. Although the same information is presented in Figs. 10 and 11, the gain plots are easier to understand and use.

The angle gain plot reflects the basic construction rule of the root locus, *i.e.*, the angle criterion of (7). As a result, the angle gain plot is symmetric about the $180°(= -180°)$ line. Furthermore, the angle criterion dictates that the eigenvalues must lie on the real axis or be complex conjugates. Thus, a pair of complex conjugate eigenvalues is shown as a single curve in the magnitude gain plot with corresponding angles symmetrically configured about the 180° line in the angle gain plot. As k varies, the complex conjugate eigenvalues may become distinct real eigenvalues, causing their angles to become equal (at a multiple of 180°) and permitting their magnitudes to differ.

The magnitude gain plot shows the presence of two open-loop poles with magnitudes 1 and 2 as $k \to 0$. It also shows a single finite transmission zero with magnitude 3 and an infinite

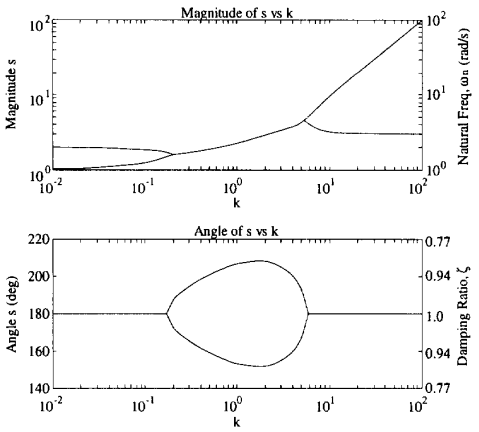

Fig. 11. Magnitude and angle gain plots of (1).

transmission zero as $k \to \infty$. At low gain, the angle gain plot indicates that the two open-loop poles are located in the left-half plane since they have angles of 180°. Furthermore, the angle gain plot shows that there are two asymptotes of 180° (corresponding to the finite and infinite transmission zeros) as $k \to \infty$.

The gain plots highlight the break points corresponding to points where branches leave or enter the real axis of the root locus. For example, these break points occur at $k \approx 0.17$ and at $k \approx 5.83$. Between these break points the angle gain plot indicates that the loci of the two branch points are not on the real axis and the corresponding single curve of the magnitude gain plot confirms that the trajectories are those of a complex conjugate pair.

IV. Properties of Gain Plots

The gain plots highlight several important stability and performance features of the closed-loop system. Stability may be determined from the angle gain plot by noting if the angle of an eigenvalue meets the following criterion:

$$180°(2m+1) - 90° < |\theta| < 180°(2m+1) + 90°, \quad m = 0, \pm 1, \pm 2, \ldots \tag{12}$$

corresponding to a location in the second and third quadrants of the complex plane. For the case $m = 0$, (12) simplifies to

$$90° < \theta < 270°. \tag{13}$$

This range is shown in the shaded region in Fig. 12(b). Since the angle gain plot of Fig. 11(b) satisfies (13), the closed- loop system is stable for the gain range depicted $(10^{-2} < k < 10^2)$ and, more generally, for all positive gains.

Performance measures are presented directly by the gain plots. In particular, for complex conjugate eigenvalues the natural frequency, ω_n, is the magnitude shown in the magnitude gain plot, and the damping ratio, ζ, is

$$\zeta = -\cos\theta \tag{14}$$

where θ is the angle from the angle gain plot. As shown in Figs. 11 and 12, supplementary axes can be added to the

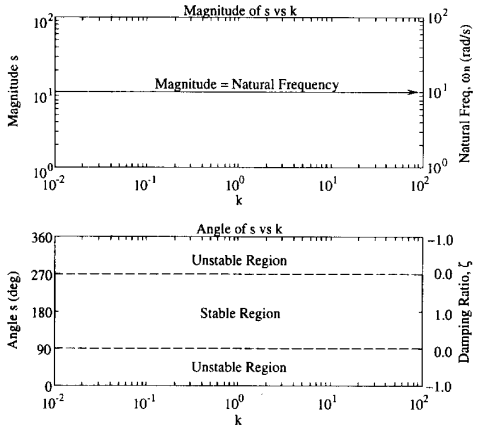

Fig. 12. Parameters in the gain plots (assuming complex conjugate poles).

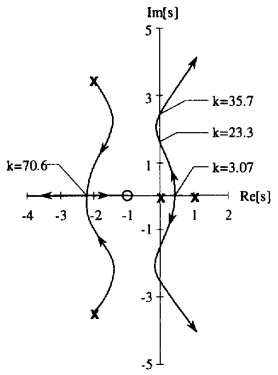

Fig. 13. Root locus plot of (15).

gain plots displaying ω_n and ζ. If the eigenvalues are on the real axis, the magnitude gain plot presents the system time constants.

Although the conventional root locus plot provides such performance information, there are several advantages of the gain plots. First, the influence of independent variable gain on ordinate (dependent) variables is exposed explicitly. Second, the performance measures of time constant or ω_n and ζ are represented directly. Thus, given a design specification for time constant or ω_n and ζ, the corresponding values of k may be determined by inspection, making the gain plots a graphic pole-placement tool that links performance and gain.

The gain plots are also well suited for determining eigenvalue sensitivity to changes in gain. The slopes of the gain plots represent the change in magnitude and angle of each eigenvalue per change in gain. This information is useful in the design of robust control systems that are less sensitive to gain variations. An in-depth treatment of sensitivity and its relation to gain plots is covered in [14].

The classical concepts of gain and phase margins are clearly depicted in the gain plots. The gain margin is the factor of gain that can be varied before the closed-loop system becomes unstable. This margin can be determined from the angle gain plot by identifying the increase/decrease in gain needed to reach the stability boundary. In principle, a system with a larger gain margin should be relatively more stable than one with a smaller gain margin. The phase margin is the largest angular interval corresponding to a constant magnitude gain for which the closed-loop system is stable. It can be determined from a modified angle gain plot where the gain is treated as complex [15].

In addition to the above advantages, the gain plots provide a unified approach for SISO and multi-input, multi-output (MIMO) systems where compensation dynamics are governed by a single scalar gain amplifying all plant inputs. The advantage of the gain plots to uniquely identify locus branches as a function of gain is of paramount importance in MIMO systems analysis, where this information is typically hidden in presenting multivariable root loci [7], [8].

V. Illustrative Example

This section presents a more complicated SISO example given by the open-loop transfer function

$$g(s) = \frac{(s+1)}{s(s-1)(s^2+4s+16)}. \tag{15}$$

(Equation (15) is studied in example A-5-3 in [5].) Fig. 13 is the root locus plot for this system embedded in the negative feedback system of Fig. 1. The root locus begins at the open-loop poles located at $s = \{0, +1, -2 \pm 2\sqrt{3}j\}$. The open-loop complex conjugate pole pair migrates to the real axis with increasing gain. One of these poles then proceeds to the finite transmission zero at $s = -1$; the other pole moves to an infinite transmission zero along an asymptote of 180°. The two real open-loop poles migrate to $s \approx 0.46$, and then break out from the real axis. As a complex conjugate pole pair, they move to the left of the imaginary axis. Subsequently, they migrate back to the right of the imaginary axis and continue toward infinite transmission zeros along asymptotes of ±60°. For a small range of k, the root locus is located completely within the left half of the complex plane, corresponding to a stable closed-loop system. This range may be found from the magnitude criterion to be

$$23.3 < k < 35.7. \tag{16}$$

Figs. 14(a) and (b) are the gain plots for the system given by (15). Information about the open-loop eigenvalues can be obtained by observing events as $k \to 0$ and shows: (1) There is an unstable set of open-loop poles at an angle of 0° having magnitudes of 0 and 1; and (2) there is a complex conjugate open-loop pole pair having magnitude 4 at angles of 120° and 240°. By inspection, these complex conjugate poles have a natural frequency of 4 rad/s and a damping ratio of 0.5; this information is "academic," since the open-loop system is unstable.

The angle gain plot shows that the system is stable only for a specific range of k, matching that given in (16). Fig. 15 is an enlargement of a section of the angle gain plot, highlighting one of the complex conjugate poles near the stable region of the closed-loop system, from which the gains may be read directly. The stability boundaries are denoted by dashed lines in accordance with the criterion presented in (12).

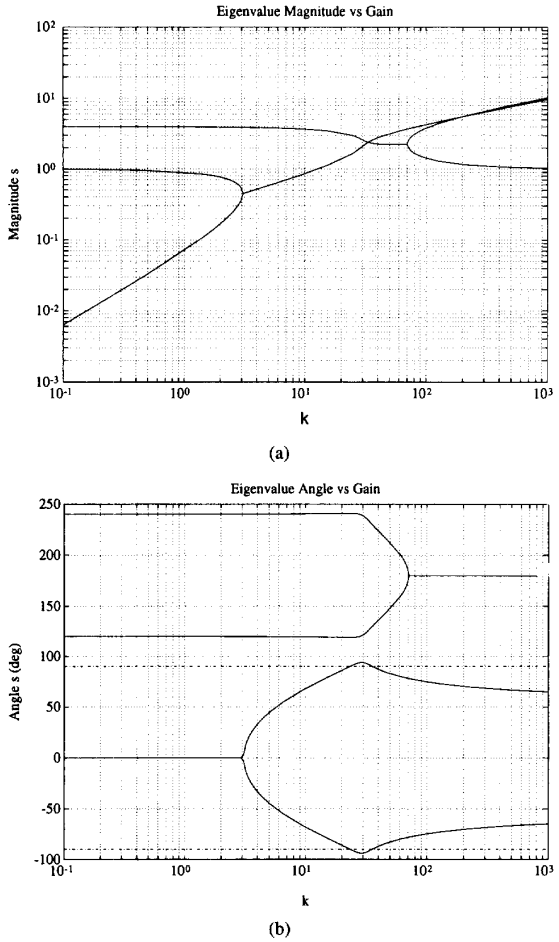

Fig. 14. (a) Magnitude gain plot of (15); (b) Angle gain plots of (15).

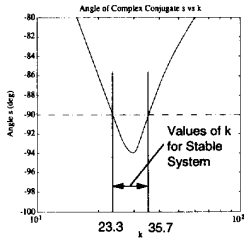

Fig. 15. Expanded angle gain plot of (15).

The high gain asymptotes of the root locus are found by examining the gain plots for large values of k. The finite zero at $s = -1$ is identified by the single pole asymptotically approaching unity magnitude at an angle of 180°. The remaining three eigenvalues asymptotically approach infinite zeros at angles ±60° and 180°. For gains higher than those reported in Figs. 14(a) and (b), these asymptotes are increasingly prominent.

Further inspection of the gain plots provides information about the closed-loop system sensitivity to changes in gain. In the example, the system is highly sensitive to gain variations

	Frequency Domain	Gain Domain
2-D	Nyquist Plot	Evans Root Locus Plot
3-D	Bode Plots	Gain Plots

Fig. 16. Quadrant representation of graphic control tools.

near $k \approx 3.1$, where the angle of the unstable pole pair changes abruptly. As $k \to \infty$: (1) The angles in the angle gain plot asymptotically approach the Butterworth configuration; and (2) the magnitudes of the eigenvalues are related to the gain via a power law relationship depicted as a straight line on the magnitude gain plot [16].

VI. Conclusion

The gain plots proposed in this paper are a set of illuminating plots that expand and enhance the design tool set of the controls engineer. By presenting eigenvalue magnitude and angle in separate graphs, the gain plots supplement the information contained in the Evans root locus, in analogy to the role the Bode plots play with respect to the Nyquist diagram. As such, the gain plots add an *explicit* third "dimension" (gain) to the Evans root locus plot, whereas the Bode plots add an *explicit* third "dimension" (frequency) to the Nyquist diagram. In the gain plots, the common axis linking magnitude and argument is gain; in the Bode plots, the common axis bridging magnitude and argument is frequency.

Fig. 16 highlights the correspondence of four graphic controls tools. The first row portrays the Nyquist diagram and the Evans root locus spanning a two-dimensional complex plane. The second row shows the Bode plots and gain plots spanning a three-dimensional (real) space. The columns show the variable that is used to increase the dimension, i.e. frequency for Bode plots, gain for gain plots. The columns correspond to the earlier progression figures (Figs. 2 and 7) where the three-dimensional representations have been removed. The four tools identified in Fig. 16 are tightly connected and are all valuable for stability and performance evaluation.

The gain plots enhance the root locus by explicitly portraying the relationship between the gain and the location of each eigenvalue whose trajectories are mapped by the root locus. The enhancement enables the control designer to identify, by observation, an eigenvalue location with a specific gain, and hence directly view the influence of gain on stability as well as on system performance. Furthermore, the gain plots provide a direct measure of root sensitivity. The change in eigenvalue magnitude and angle per change in gain is indicated by the slope of the gain plots. This measure of sensitivity highlights the "cost" of selecting eigenvalue locations corresponding to specific gain values, and provides the designer with a graphic means to assess control system robustness.

Many similarities and differences exist between the root locus and the gain plots. For example, both the root locus plot and the gain plots can be drawn for systems with transportation lags or dead time. Unlike the root locus plot, the gain plots explicitly highlight open-loop poles near or at transmission zeros. These poles are depicted as horizontal lines indicat-

ing constant magnitude and angle for all gains. In the root locus plot pole-zero cancellations are normally camouflaged. Explicit sketching rules exist for the root locus plot. Although only an incomplete set of sketching rules has been found for the gain plots, their utility may be limited given the wide availability of computer graphics.

Further work is necessary to develop intuitive geometric relationships between the Bode plots that present open-loop information and the gain plots that present closed-loop information (for $k \neq 0$). The Nichols chart may provide the appropriate connection. It presents the relationship between the frequency response of the open-loop system and that of the closed-loop system. In so doing, it displays four dimensions of information (i.e., open and closed-loop gain and magnitude) in a two-dimensional format where ω is the implicit variable. The Nichols chart is challenging to generate and comprehend; however, it does provide a bridge between open-loop and closed-loop systems in the frequency domain. Other controls tools, such as the generalized Bode diagrams [11], [12], can be used to geometrically link the open-loop and closed-loop regimes as well as the frequency and gain domains.

We have introduced the concept of gain plots in undergraduate and graduate controls courses and in a faculty enhancement workshop. The concept and its development have met with tremendous success. Proof of student excitement is evident in their endorsement of gain plots for a variety of control system analysis and design problems. Common student feedback is that "the gain plots give you a feeling of what's going on." As educators, we value the gain plots as offering an alternative and complementary representation of the classical graphic tools. For control system design, we see the gain plots being valuable for SISO and MIMO systems where the influence of any scalar parameter can be explored.

In closing, controls engineers have historically embraced powerful graphic design methods with striking success. These methods supply significant insight, permitting rapid system analysis and synthesis. This paper promotes the gain plots as a graphic control systems design tool. It motivates these plots via a global perspective that ties together important classical control tools. The gain plots provide a broad spectrum of information about the closed-loop control system, including stability, performance, and robustness attributes.

ACKNOWLEDGMENT

The authors would like to thank Professors R. C. Dorf (University of California, Davis) and H. M. Paynter (Massachusetts Institute of Technology, Emeritus) for their enthusiastic support. They also wish to thank Dr. D. T. McRuer (Systems Technology) and Professor R. F. Stengel (Princeton University) for identifying the earlier, very relevant work of [11], [12]. Furthermore, the authors are grateful to the participants of the 1993 Faculty Enhancement Workshop "A Unified Classical/Modern Approach for Undergraduate Control Education" for their valuable comments.

REFERENCES

[1] W. R. Evans, "Graphical analysis of control systems,"*Trans. Amer. Inst. of Elect. Eng.*, vol. 67, 1948, pp. 547–551.
[2] W. R. Evans, "Control system synthesis by root locus method," *Trans. Amer. Inst. of Elect. Eng.*, vol. 69, 1950, pp. 1–4.
[3] R. C. Dorf, *Modern Control Systems*. Sixth edition, Reading, MA: Addison-Wesley, 1992.
[4] B. C. Kuo, *Automatic Control Systems*. Fifth edition, Englewood Cliffs, NJ: Prentice Hall, 1991.
[5] K. Ogata, *Modern Control Engineering*. 2nd ed., Englewood Cliffs, NJ: Prentice-Hall, 1990.
[6] W. J. Palm III, *Control Systems Engineering*. New York: John Wiley, 1986.
[7] T. R. Kurfess and M. L. Nagurka, "Understanding the root locus using gain plots," *IEEE Cont. Syst. Mag.*, vol. 11, Aug. 1991, pp. 37–40.
[8] M. L. Nagurka and T. R. Kurfess, "An alternate geometric perspective on MIMO systems" *ASME J. Dynamic Syst. Measurement and Cont.*, vol. 115, pp. 538–543, Sept. 1993.
[9] H. Nyquist, "Regeneration theory," *Bell Syst. Tech. J.*, vol. 11, 1932, pp 126–147.
[10] H. W. Bode, "Relations between attenuation and phase in feedback amplifier design," *Bell Syst. Tech. J.*, vol. 19, 1940, pp. 421–454.
[11] D. T. McRuer, I. Ashkenas, and D. Graham, *Aircraft Dynamics and Automatic Control*. Princeton, NJ: Princeton University Press, 1973.
[12] D. T. McRuer, "Unified analysis of linear feedback systems," *ASD Tech. Rep. 61–118*, Wright-Patterson Air Force Base, OH, 1961.
[13] R. H. Cannon Jr., *Dynamics of Physical Systems*. New York: McGraw-Hill, 1967.
[14] T. R. Kurfess and M. L. Nagurka, "A geometric representation of root sensitivity," *ASME J. Dynamic Syst., Measurement and Cont.*, accepted for publication (expected June 1994).
[15] M. L. Nagurka and T. R. Kurfess, "Gain and phase margins of SISO systems from modified root locus plots," *IEEE Cont. Syst. Mag.*, vol. 12, June 1992, pp. 123–127.
[16] T. R. Kurfess and M. L. Nagurka, "Foundations of classical control theory with reference to eigenvalue geometry," *J. Franklin Inst.*, vol. 330, Mar. 1993, pp. 213–227.

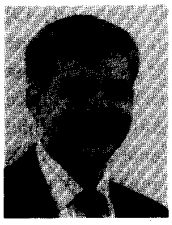

Thomas R. Kurfess received his S.B., S.M., and Ph.D. degrees in mechanical engineering from Massachusetts Institute of Technology in 1986, 1987, and 1989, respectively. He also earned an S.M. degree in electrical enginering and computer science from Massachusetts Institute of Technology in 1988.

Following graduation, he joined the faculty in the departments of Mechanical Engineering and Engineering and Public Policy at Carnegie Mellon University. His research interests lie in the area of control and manufacturing, with special emphasis on precision engineering.

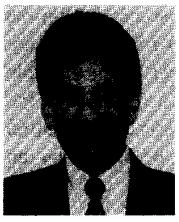

Mark L. Nagurka received his B.S. and M.S. degrees in mechanical engineering and applied mechanics from the University of Pennsylvania in 1978 and 1979, respectively, and his Ph.D. degree from Massachusetts Institute of Technology in 1983.

Following graduation, he joined the faculty in the Department of Mechanical Engineering at Carnegie Mellon University. The focus of his work is the integration of optimal control methods into practical mechanical systems, with emphasis on robotic and biomechanical systems.